

A Modified Gysel Power Divider With Arbitrary Power Dividing Ratio

Shiyong Chen^{*}, Guoqiang Zhao, and Yantao Yu

Abstract—A modified Gysel power divider with arbitrary power dividing ratio is proposed in this letter. The power dividing ratio of the proposed circuit is determined by both the electrical lengths and characteristic impedances of transmission lines. The proposed circuit is analyzed based on transmission line theory, and design equations are derived. For verification, two prototypes operating at 2 GHz with power dividing ratios of 1 : 1 and 4 : 1 are designed, fabricated and measured, respectively. The measured results are in good agreements with the simulated ones.

1. INTRODUCTION

Microwave power dividers are one kind of important components and have been widely utilized in microwave circuits and systems [1]. As a Gysel power divider has advantages of high power capacity and easy layout, a lot of related research works have been reported: single or dual band operation [2–6] improving operating bandwidth [7–10] and out-of-phase feature [11–13]. To reduce the size of microwave sub-systems, Wilkinson or Gysel power dividers with filtering response have been introduced in [14–18]. For a single or dual band Gysel power divider, there are two methods to realize the required power dividing ratio between output loads. Firstly, the power dividing ratio can be achieved by designating different characteristic impedances of transmission lines with the same electrical lengths [2–5, 7–13]. However, physical realization is very difficult for the power divider with large power dividing ratio. Moreover, the power distribution ratio of the Gysel power divider is determined by only the electrical lengths of transmission lines with uniform characteristic impedance [6] as shown in Figure 1(a). For the Gysel power divider discussed above, design flexibility is limited to some extent, as purely a set of transmission line parameters (the characteristic impedances or the electrical lengths) are utilized to obtain the required power dividing ratio.

Different from the reported works, the power dividing ratio of the proposed Gysel power divider is controlled by two sets of transmission line parameters, which help to design the power divider more flexibly. The proposed circuit is analyzed, and design equations are derived. Experimental results have verified the concept.

2. THEORY ANALYSIS

The configuration of the proposed Gysel power divider is shown in Figure 1(b). It consists of five transmission line sections with the characteristic impedances of Z_1 , Z_2 and Z_3 , and two isolation resistors of R_1 and R_2 . The power dividing ratio between two output loads is defined as $K^2 = P_3/P_2$. When the input port is fed by microwave signal, the electromagnetic energy is only transmitted into two output loads, and the isolation resistors can be regarded as short circuited. Therefore, the original circuit can

Received 17 May 2018, Accepted 21 June 2018, Scheduled 29 June 2018

^{*} Corresponding author: Shiyong Chen (chensy@cqu.edu.cn).

The authors are with the College of Communication Engineering, Chongqing University, Chongqing 400044, China.

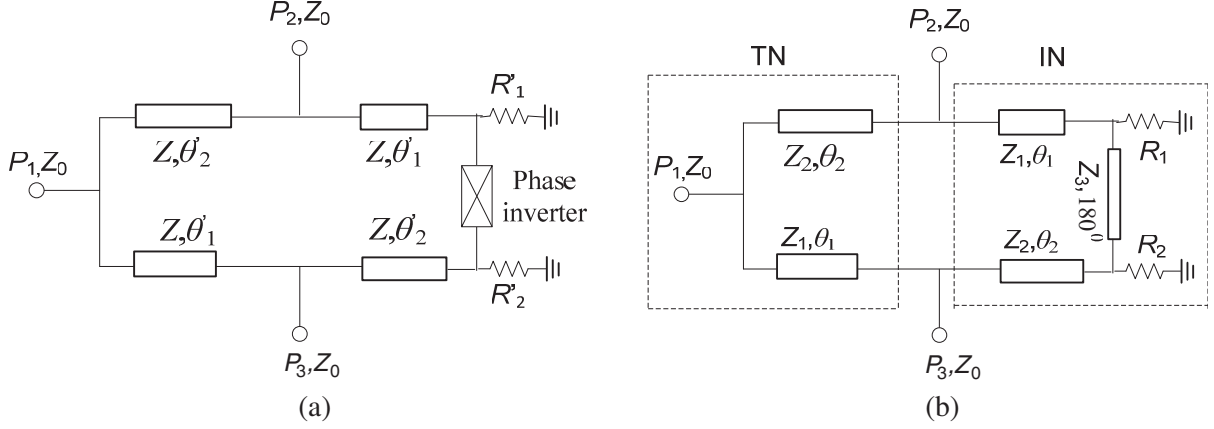


Figure 1. Topology of power divider. (a) Gysel power divider in [6]. (b) Proposed Gysel power divider.

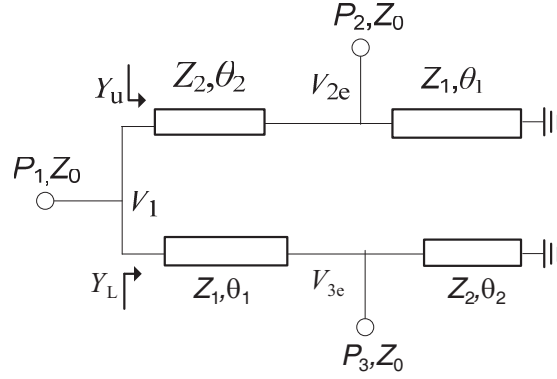


Figure 2. Even-mode equivalent circuit.

be converted into an even mode equivalent circuit, as shown in Figure 2. Based on the even-mode voltages V_{2e} and V_{3e} , the designated power dividing ratio can be written as

$$\frac{P_3}{P_2} = \frac{|V_{3e}|^2/Z_0}{|V_{2e}|^2/Z_0} = K^2 \quad (1)$$

which indicates that $V_{3e} = KV_{2e}$ as the input port is excited.

The node voltage of V_1 shown in Figure 2 is described by using $ABCD$ parameters as

$$V_1 = (\cos \theta_2 + Z_2 Y_1 \sin \theta_2 \text{ctg} \theta_1) V_{2e} + j Z_2 Y_0 \sin \theta_2 V_{2e} \quad (2)$$

$$V_1 = (\cos \theta_1 + Z_1 Y_2 \sin \theta_1 \text{ctg} \theta_2) V_{3e} + j Z_1 Y_0 \sin \theta_1 V_{3e} \quad (3)$$

where $Y_2 = 1/Z_2$, $Y_1 = 1/Z_1$ and $Y = 1/Z_0$.

By substituting $V_{3e} = KV_{2e}$ into Eq. (3) and equating the real and imaginary parts of Eqs. (2) and (3), the power dividing ratio of K^2 can be expressed as

$$K^2 = \left(\frac{Z_2 \sin \theta_2}{Z_1 \sin \theta_1} \right)^2 \quad (4)$$

From Eq. (4), it can be seen that the power dividing ratio can be determined by both the characteristic impedances and electrical lengths of transmission lines. Different combinations of (Z_2/Z_1) and $(\sin \theta_2/\sin \theta_1)$ can be adopted to realize the specific power dividing ratio, which increase design agility.

By applying transmission line theory, the input admittances of Y_u and Y_L shown in Figure 2 can be expressed, respectively, as

$$Y_u = Y_2 \frac{Y_0 - jY_1 \text{ctg}\theta_1 + jY_2 \tan \theta_2}{Y_2 + j(Y_0 - jY_1 \text{ctg}\theta_1) \tan \theta_2} \quad (5)$$

$$Y_L = Y_1 \frac{Y_0 - jY_2 \text{ctg}\theta_1 + jY_1 \tan \theta_1}{Y_1 + j(Y_0 - jY_2 \text{ctg}\theta_1) \tan \theta_1} \quad (6)$$

To satisfy the matching condition of the input port, the sum of Y_u and Y_L should be equal to Y_0 .

$$Y_U + Y_L = Y_0 \quad (7)$$

As transmission lines are assumed lossless, and the branch circuits have a common voltage node of V_1 , the real parts of Y_u and Y_L can be described as

$$\text{Re}(Y_u) = \frac{1}{1 + K^2} Y_0 \quad (8)$$

$$\text{Re}(Y_L) = \frac{K^2}{1 + K^2} Y_0 \quad (9)$$

To substitute (8) and (4) into (5), the characteristic impedance of Z_1 and Z_2 can be derived, respectively, as

$$Z_1 = \frac{Z_0 \sqrt{1 + K^2 - K^2 (\cos \theta_1 + \cos \theta_2 / K)^2}}{K \sin \theta_1} \quad (10)$$

$$Z_2 = \frac{Z_1 K \sin \theta_1}{\sin \theta_2} \quad (11)$$

The $ABCD$ parameters of transmission network (TN) and isolation network (IN) shown in Figure 1(b) can be written as

$$\begin{bmatrix} A_{\text{TN}} & B_{\text{TN}} \\ C_{\text{TN}} & D_{\text{TN}} \end{bmatrix} = \begin{bmatrix} \cos \theta_2 & jZ_2 \sin \theta_2 \\ jY_2 \sin \theta_2 & \cos \theta_2 \end{bmatrix} \begin{bmatrix} 1 & 0 \\ Y_0 & 1 \end{bmatrix} \begin{bmatrix} \cos \theta_1 & jZ_1 \sin \theta_1 \\ jY_1 \sin \theta_1 & \cos \theta_1 \end{bmatrix} \quad (12)$$

$$\begin{bmatrix} A_{\text{IN}} & B_{\text{IN}} \\ C_{\text{IN}} & D_{\text{IN}} \end{bmatrix} = \begin{bmatrix} \cos \theta_1 & jZ_1 \sin \theta_1 \\ jY_1 \sin \theta_1 & \cos \theta_1 \end{bmatrix} \begin{bmatrix} 1 & 0 \\ G_1 & 1 \end{bmatrix} \begin{bmatrix} -1 & 0 \\ 0 & -1 \end{bmatrix} \begin{bmatrix} 1 & 0 \\ G_2 & 1 \end{bmatrix} \begin{bmatrix} \cos \theta_2 & jZ_2 \sin \theta_2 \\ jY_2 \sin \theta_2 & \cos \theta_2 \end{bmatrix} \quad (13)$$

where $G_1 = 1/R_1$, $G_2 = 1/R_2$.

As discussed in [2], the perfect isolation condition between two output ports means that the sum of B_{TN} and B_{IN} is equal to zero.

$$B_{\text{TN}} + B_{\text{IN}} = 0 \quad (14)$$

By substituting Eqs. (12) and (13) into Eq. (14), the isolation resistors R_1 and R_2 must satisfy the following equation.

$$Y_0 = G_1 + G_2 \quad (15)$$

As the characteristic impedance Z_3 of phase inverter does not affect the port matching, it can be freely selected. The whole power dividing ratio of K^2 is equal to the product of $(Z_2/Z_1)^2$ and $(\sin \theta_2 / \sin \theta_1)^2$. Proper electrical lengths of θ_2 and θ_1 can be firstly chosen to realize a part of K^2 , and then Z_1 and Z_2 are calculated based on formulas (10) and (11), which contribute to the left proportion of K^2 .

3. DISCUSSION

If $Z_1 = Z_2$, by substituting Eq. (4) into Eq. (10), it is interesting to find that the characteristic impedance can be expressed as

$$Z_1 = Z_2 = Z_0 \sqrt{2 - 2 \text{ctg}\theta_1 \text{ctg}\theta_2} \quad (16)$$

which is identical to the characteristic impedance expression described in [6].

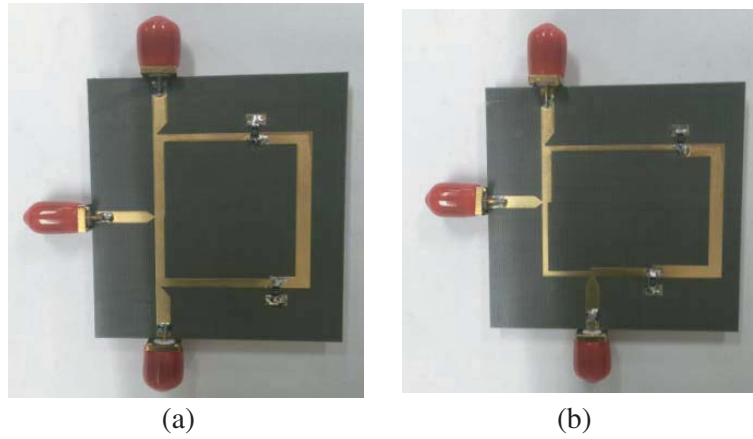


Figure 3. Photographs of fabricated circuits. (a) $K^2 = 1$. (b) $K^2 = 4$.

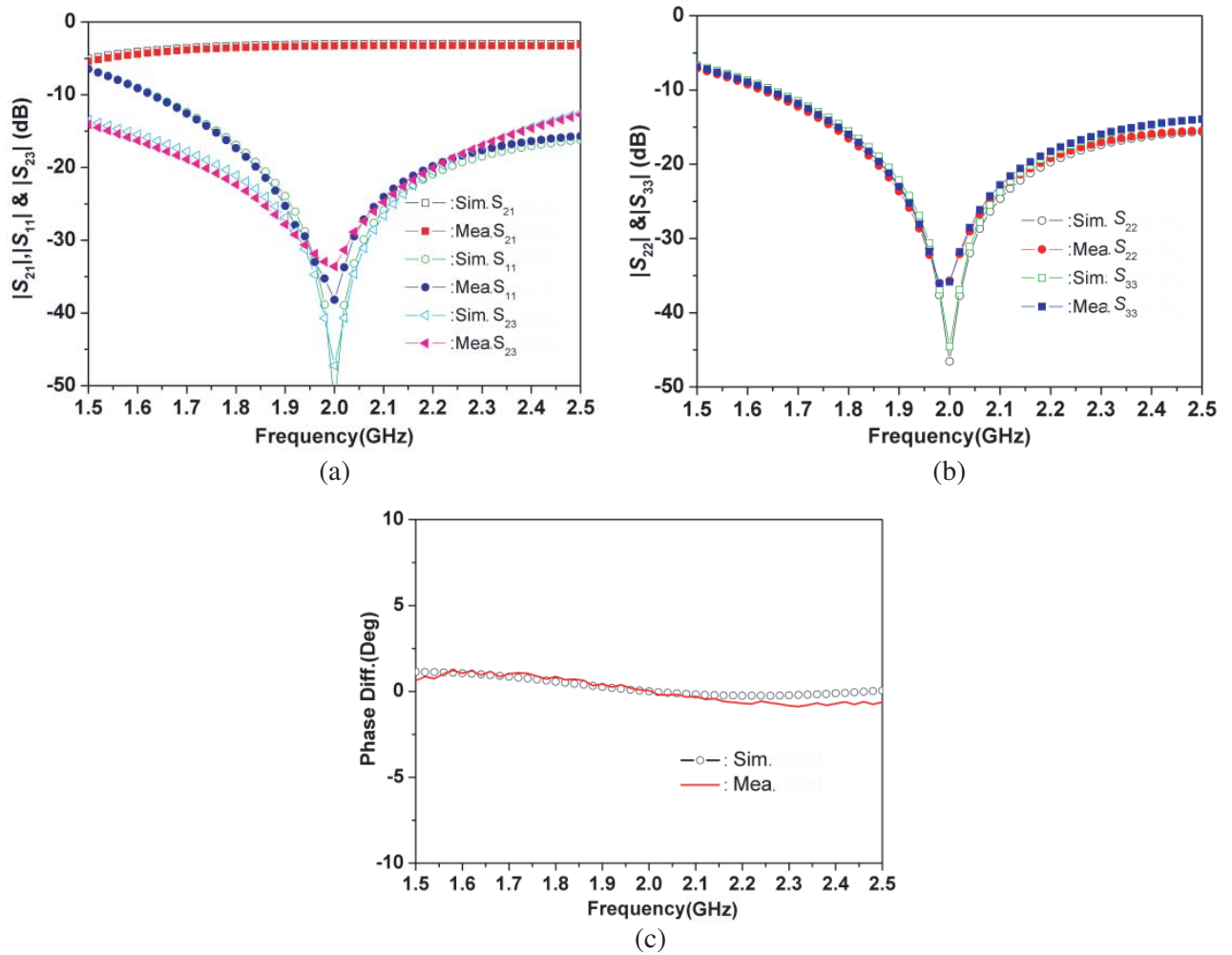


Figure 4. Simulated and Measured results for $K^2 = 1$. (a) S_{11} , S_{21} , S_{23} . (b) S_{22} , S_{33} . (c) $\angle S_{21} - \angle S_{31}$.

Moreover, if $\theta_1 = \theta_2 = 90^\circ$, in the same way, the characteristic impedances can be rewritten, respectively, as

$$Z_1 = Z_0 \sqrt{\frac{1+K^2}{K^2}} \tag{17}$$

$$Z_2 = K Z_1 \tag{18}$$

which is corresponding to design formula of the Gysel power divider with terminations of Z in [2]. Therefore, the power dividers with terminations of Z in [2] and [6] can be regarded as special cases of the proposed one.

In addition, if only $\theta_2 = 90^\circ$, formulas (10) and (11) can be simplified as

$$Z_1 = Z_0 \sqrt{1 + \frac{1}{K^2 \sin^2 \theta_1}} \tag{19}$$

$$Z_2 = Z_0 \sqrt{1 + K^2 \sin^2 \theta_1} \tag{20}$$

From Eqs. (19) and (20), physical realization of the proposed power divider with extremely high power dividing ratio is very easy if we choose a proper value of θ_1 to make $K^2 \sin^2 \theta_1$ approximately equal to 1.

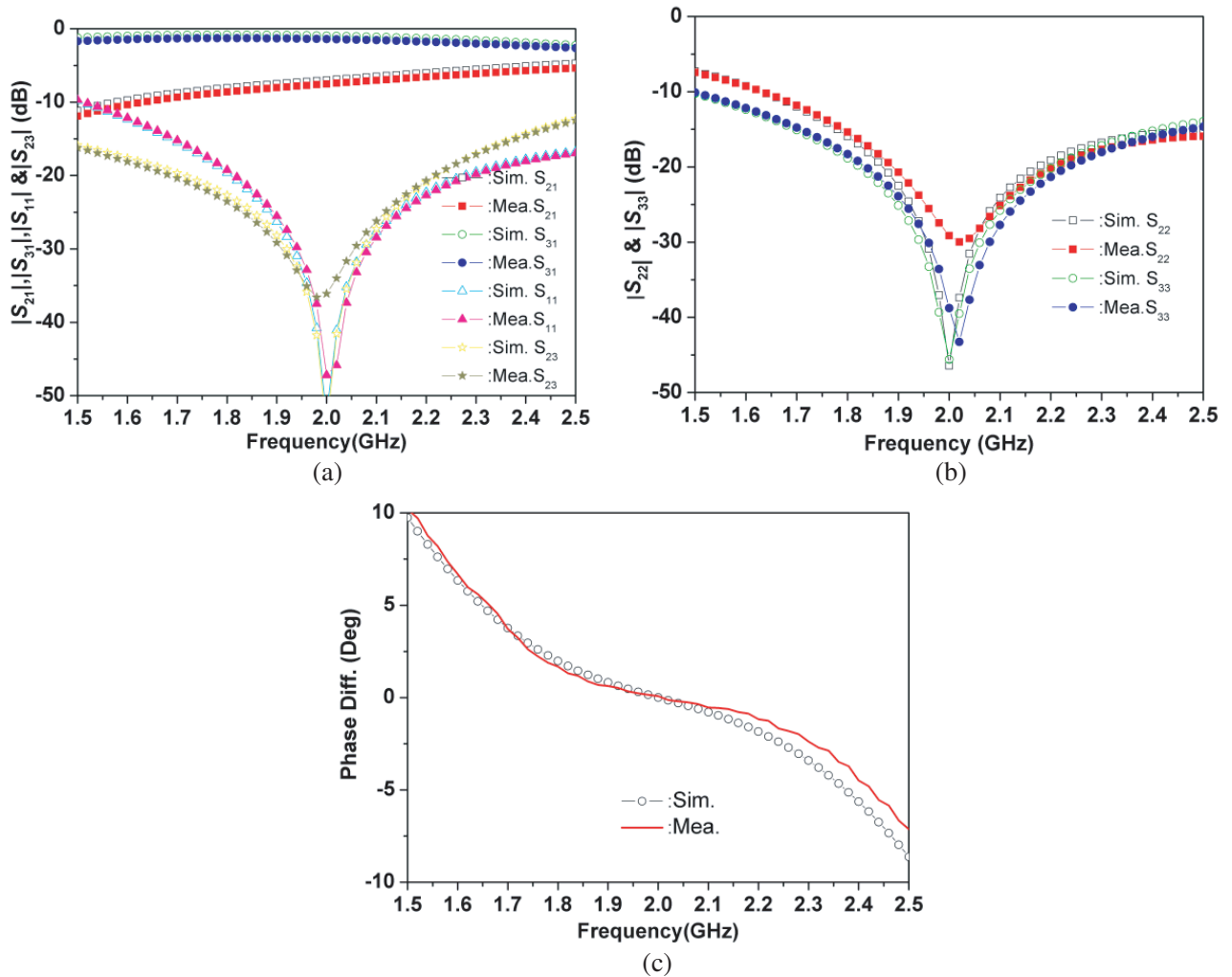


Figure 5. Simulated and Measured results for $K^2 = 4$. (a) $S_{11}, S_{21}, S_{31}, S_{23}$. (b) S_{22}, S_{33} . (c) $\angle S_{21} - \angle S_{31}$.

4. EXPERIMENTAL RESULTS

To verify the concept, two prototypes operating at 2 GHz with $K^2 = 1$ and $K^2 = 4$ have been designed, respectively. The relative dielectric constant and the thickness of the substrate are 2.65 and 1 mm. For the first example ($K^2 = 1$), $\theta_1 = 70^\circ$ and $\theta_2 = 60^\circ$ are selected. The calculated characteristic impedances are $Z_1 = 60.5 \Omega$ and $Z_2 = 65.5 \Omega$. For the second one ($K^2 = 4$), $\theta_1 = 45^\circ$ and $\theta_2 = 90^\circ$ are selected. The corresponding characteristic impedances are $Z_1 = 61.2 \Omega$ and $Z_2 = 86.6.7 \Omega$. In addition, $Z_3 = 50 \Omega$ and $R_1 = R_2 = 100 \Omega$ for two experimental circuits are chosen. Figure 3 shows photographs of two fabricated prototypes. The experimental circuits were measured by the vector network analyzer. The simulated and measured results for $K^2 = 1$ are shown in Figure 4. It can be observed that the measured $|S_{21}|$ and $|S_{31}|$ are about 3.55 dB at 2 GHz. The measured operating bandwidth based on $|S_{11}| < 20$ dB is about 17%. The measured isolation is better than 20 dB in the range of 1.74 to 2.18 GHz. Figure 4(c) shows the phase differences between two output ports, and the measured maximum phase difference is about 1° from 1.5 to 2.5 GHz. Moreover, the simulated and measured results for $K^2 = 4$ are shown in Figure 5. It can be seen that the measured $|S_{21}|$ and $|S_{31}|$ are 7.14 and 1.25 dB at the center frequency. The measured $|S_{11}|$ is greater than 20 dB from 1.83 to 2.27 GHz. The measured isolation is larger than 20 dB from 1.71 to 2.25 GHz. In addition, the simulated and measured phase differences are shown in Figure 5(c). The measured maximum phase imbalance is about 1.6° in the range of 1.8 to 2.2 GHz. The measured results are in good agreements with the simulated ones.

5. CONCLUSION

A modified Gysel power divider with arbitrary power dividing ratio is presented in this letter. The power division ratio can be achieved by controlling both the electrical lengths and characteristic impedances of transmission lines. The circuit is analyzed, and design equations are given. The measured results of two prototypes have verified the idea. The proposed circuit can be utilized in related applications with power dividing requirements.

ACKNOWLEDGMENT

This work was financially supported by the National Natural Science Foundation of China (No. 61571069 and No. 61471072) and in part by the Fundamental Research Funds for the Central Universities (No. 106112017CDJQJ168817).

REFERENCES

1. Wu, Y. L., L. X. Jiao, Z. Zhuang, and Y. A. Liu, "The art of power dividing: A review for state-of-the-art planar power dividers," *China Communications*, Vol. 14, No. 5, 1–16, 2017.
2. Wu, Y. L. and Y. A. Liu, "A modified Gysel power divider of arbitrary power ratio and real terminated impedances," *IEEE Microw. Wirel. Compon. Lett.*, Vol. 21, No. 11, 601–603, 2011.
3. Sun, Z., L. Zhang, Y. Liu, and X. Tong, "Modified Gysel power divider for dual-band applications," *IEEE Microw. Wirel. Compon. Lett.*, Vol. 21, No. 1, 16–18, 2011.
4. Sun, Z., L. Zhang, Y. P. Yan, and H. W. Yang, "Design of unequal dual-band Gysel power divider with arbitrary termination resistance," *IEEE Trans. Microw. Theory Tech.*, Vol. 59, No. 8, 1955–1962, 2011.
5. Park, M. J. and B. Lee, "A dual-band Gysel power divider with the even-mode input extension stub lines," *Microwave Opt. Technol. Lett.*, Vol. 53, No. 6, 1213–1216, 2011.
6. Lin, F., Q. X. Chu, and S. W. Wong, "A novel Gysel power divider design with uniform impedance transmission lines for arbitrary power-dividing ratios," *Journal of Electromagnetic Waves and Applications*, Vol. 27, No. 2, 242–249, 2012.
7. Oraizi, H. and A. R. Sharifi, "Optimum design of a wideband two-way Gysel power divider with source to load impedance matching," *IEEE Trans. Microw. Theory Tech.*, Vol. 57, No. 9, 2238–2248, 2009.

8. Oraizi, H. and A. R. Sharifi, "Optimum design of asymmetrical multi-section two-way power dividers with arbitrary power division and impedance matching," *IEEE Trans. Microw. Theory Tech.*, Vol. 59, No. 6, 1478–1490, 2011.
9. Lin, F., Q. X. Chu, Z. Gong, and Z. Lin, "Compact broadband Gysel power divider with arbitrary power-dividing ratio using microstrip/slotline phase inverter," *IEEE Trans. Microw. Theory Tech.*, Vol. 60, No. 5, 1226–1234, 2012.
10. Zhang, H., X.-W. Shi, F. Wei, and L. Xu, "Compact wideband Gysel power divider with arbitrary power division based on patch type structure," *Progress In Electromagnetics Research*, Vol. 119, 395–406, 2011.
11. Dai, G., X. Wei, E. Li, and M. Xia, "Novel dual-band out-of-phase power divider with high power-handling capability," *IEEE Trans. Microw. Theory Tech.*, Vol. 60, No. 8, 2403–2409, 2012.
12. Lu, Y. L., G.-L. Dai, X. Wei, and E. Li, "A broadband out-of-phase power divider for high power applications using through ground via (TGV)," *Progress In Electromagnetics Research*, Vol. 137, 653–667, 2013.
13. Chen, S. Y., Y. T. Yu, and M. C. Tang, "Planar out-of-phase Gysel power divider with high power splitting ratio," *Electron. Lett.*, Vol. 51, No. 24, 2010–2012, 2015.
14. Wu, Y. L., Z. Zhuang, and Z. Ghassemlooy, "Generalized dual-band unequal filtering power divider with independently controllable bandwidth," *IEEE Trans. Microw. Theory Tech.*, Vol. 65, No. 10, 3838–3848, 2017.
15. García, R. G., D. Psychogiou, and D. Peroulis, "Fully-tunable filtering power dividers exploiting dynamic transmission-zero allocation," *IET Microw. Antennas Propag.*, Vol. 11, No. 3, 378–385, 2017.
16. Tang, C. W. and J. T. Chen, "A design of 3-dB wideband microstrip power divider with an ultra-wide isolated frequency band," *IEEE Trans. Microw. Theory Tech.*, Vol. 64, No. 6, 1806–1811, 2016.
17. Jiao, L. X., Y. L. Wu, and A. A. Kishk, "Planar balanced-to-unbalanced in-phase power divider with wideband filtering response and ultra-wideband common-mode rejection," *IEEE Trans. Circuits Syst. I, Reg. Papers*, Vol. 65, No. 6, 1875–1886, 2018.
18. Wang, K. X., X. Y. Zhang, and B. J. Hu, "Gysel power divider with arbitrary power ratios and filtering responses using coupling structure," *IEEE Trans. Microw. Theory Tech.*, Vol. 62, No. 3, 431–440, 2014.